ENVIRONMENTAL RESEARCH
LETTERS

PURPOSE-LED PUBLISHING™

LETTER • OPEN ACCESS

Projecting atmospheric N_2O rise until the end of the 21st century: an Earth System Model study

To cite this article: M De Sisto *et al* 2024 *Environ. Res. Lett.* **19** 124036

IOP Publishing Environ. Res. Lett. 19 (2024) 124036 https://doi.org/10.1088/1748-9326/ad8c6c

ENVIRONMENTAL RESEARCH
LETTERS

LETTER

Projecting atmospheric N_2O rise until the end of the 21st century: an Earth System Model study

M De Sisto[1,2,*], **C Somes**[3], **A Landolfi**[3] **and A H MacDougall**[1]

[1] St. Francis Xavier University, Antigonish, NS, Canada
[2] Faculty of Engineering and Applied Science, Memorial University of Newfoundland, St. John's, NL, Canada
[3] GEOMAR Helmholtz Centre for Ocean Research Kiel, Kiel, Germany
[*] Author to whom any correspondence should be addressed.

E-mail: mdesisto@stfx.ca

Keywords: projecting atmospheric N_2O concentrations, coupled terrestrial and ocean N_2O dynamics, N_2O emissions

OPEN ACCESS

RECEIVED
6 September 2023

REVISED
22 October 2024

ACCEPTED FOR PUBLICATION
29 October 2024

PUBLISHED
12 November 2024

Abstract

Nitrous Oxide (N_2O) is a potent greenhouse gas with a centennial-scale lifetime that contributes significantly to global warming. It is emitted from natural and anthropogenic sources. In nature, N_2O is released mainly from nitrification and denitrification from the ocean and terrestrial systems. The use of agricultural fertilizers has significantly increased the emission of N_2O in the past century. Here we present, to our knowledge, the first coupled ocean and terrestrial N_2O modules within an Earth System Model. The coupled modules were used to simulate the six Shared Socioeconomic Pathways (SSPs) scenarios with available nitrogen fertilizer inputs. Our results are compared to projections of atmospheric N_2O concentrations used for SSPs scenario experiments. Additionally, an extra set of simulations were prescribed with emulated N_2O concentrations available as input in Shared Socioeconomic Pathways scenarios. We report four main drivers for terrestrial N_2O uncertainties: atmospheric temperature, agricultural fertilizer input, soil denitrification and agricultural model dynamics. We project an atmospheric N_2O concentration range from 401 to 418 ppb in six SSPs simulations with a robust lack of sensitivity to equilibrium climate sensitivity. We found a large difference between our low emission scenarios N_2O concentrations by 2100 compared to the concentration provided for SSPs experiments. This divergence is likely explained by strong mitigation assumptions that were not accounted for in this study, which would require a substantial decrease of agricultural N_2O emissions. The coupled model and the simulations prescribed with N_2O concentrations showed a difference between −0.02 and 0.09 °C by 2100. Our model simulation shows a lack of sensitivity to climate mitigation efforts projecting similar N_2O concentration in low and high mitigation scenarios, that could indicate the need of further development of agricultural model dynamics. Further improvements in Earth system models should focus on the impact of oxygen decline on N_2O dynamics in the ocean and the representation of anaerobic soils and agricultural dynamics on land, including mitigation methods on nitrogen fertilizers.

1. Introduction

Despite carbon dioxide being the largest contributor to anthropogenic climate warming, other naturally occurring but anthropogenically produced greenhouse gasses, such as methane and nitrous oxide (N_2O), also contribute substantially to warming (Montzka *et al* 2011, Tian *et al* 2016, IPCC 2022). N_2O is a powerful greenhouse gas with a 120 years lifetime (Prather *et al* 2015) and a strong global warming potential. In nature, N_2O is released as an intermediate product during nitrification and denitrification in terrestrial and aquatic ecosystems, both of which are mediated by microorganisms (Fowler *et al* 2013). Total N_2O emissions are enhanced by anthropogenic activities including agriculture,

industry (chemical processing), wastewater management and fossil fuel combustion (Tian *et al* 2016, IPCC 2022).

A large portion of atmospheric N_2O is photolyzed at ultraviolet wavelengths around 200 nm, in the stratosphere. The photodissociation of N_2O is important for the photochemical balance of ozone and is the major contributor to NO_x species in the stratosphere (Nishida *et al* 2004). The lifetime of N_2O is therefore associated to the photolysis rate of N_2O in the stratopshere and is expected to decrease with higher N_2O abundances (Prather *et al* 2023).

In the oceans, N_2O production can occur both in the water column and marine sediments (Landolfi *et al* 2017) and is sensitive to the rate of remineralization of organic matter. The reduction of oxygen and expansion of oxygen minimum zones are expected to increase the oceanic N_2O production (Landolfi *et al* 2017, Yang *et al* 2020). Conversely, N_2O is consumed in oxygen depleted waters, which could compensate the aforementioned increased production, albeit likely to a small extent given the small volume of oxygen deficient waters. Marine N_2O is released into the atmosphere where N_2O rich waters resurface and diffuse to the atmosphere (Yang *et al* 2020). On land, denitrification has been identified as the main pathways of nitrogen loss for agricultural soils and natural ecosystems. Combined global marine and terrestrial denitrification estimates range from 220 to 570 Tg N yr^{-1} (Scheer *et al* 2020). In terrestrial systems, denitrification estimates range from 100 to 250 Tg N yr^{-1} most of which occurs in soils and half of it on agricultural land followed by lakes, rivers and groundwater (Groffman 2012, Scheer *et al* 2020). Denitrification is usually found in the interface of aquatic and soil ecosystems.

Based on NOAA atmospheric measurements, N_2O concentrations reached 336 ppb in 2023 with a tropospheric growth rate of 0.71 ppb yr^{-1} (Lan *et al* 2023). This represents an increase of 24% over preindustrial concentrations (270 ppb). Emissions from agricultural activities are a major source of atmospheric N_2O (Tian *et al* 2020). Agricultural fertilizers are the primary contributor to N_2O emissions in agricultural systems. Tian *et al* (2020) estimated an increase of 31 ppb of atmospheric N_2O from 1980 to 2019 due to synthetic fertilizers and manure, nitrogen deposition from agriculture and fossil fuel burning. Various strategies have been proposed to mitigate N_2O emissions from agricultural sources. These include improving fertilizer management practices, developing best management practices for animal manure management, and utilizing cover crops and crop rotations (Hassan *et al* 2022). Additionally, a number of technologies have been developed to reduce N_2O emissions from agricultural sources, such as nitrification inhibitors, nitrification–denitrification inhibitors, and nitrification–denitrification reactors (Norton *et al* 2019, Saud *et al* 2022).

The total N_2O emissions from 2007 to 2016 were estimated to be 17.0 (12.2–23.5) TgN yr^{-1} (Tian *et al* 2020). The terrestrial sources contribute to a total of 11.3 (10.2–13.2) TgN yr^{-1} and the ocean 5.7 (3.4 to 7.2) TgN yr^{-1}. Anthropogenic emission of N_2O are estimated to be around 40% of the total. From a modelling perspective, oceanic and terrestrial N_2O emission have been represented separately in Earth system models previously (Manizza *et al* 2012, Suntharalingam *et al* 2012, Davidson and Kanter 2014, Martinez-Rey *et al* 2015, Landolfi *et al* 2017, Buitenhuis *et al* 2018, Tian *et al* 2020). The model estimates are usually constrained by the effectiveness of the model to represent denitrification and nitrification processes. The challenges include the definition of the dynamics of inland waters, estuaries, oxygen in soil and column of water. The multimodel ocean and land (no agriculture) estimate N_2O emission to be 3.4 (2.5–4.3) and 6.7 (5.3–8.1) TgN yr^{-1} (IPCC 2022).

The total anthropogenic radiative forcing of greenhouse gasses between 1960 and 2019 was 63% for CO_2, 11% for CH_4, 6% for N_2O, and 17% for the halogenated species (Canadel *et al* 2021). The future N_2O in highly uncertain given that is highly dependent on anthropogenic sources (e.g. agriculture fertilization). Martinez-Rey *et al* (2015) projected oceanic N_2O emissions from 2005 to 2100 and found a decrease from 4.03 to 3.54 TgN yr^{-1} similar to Landolfi *et al* (2017) and Battliaga and Joos (2018). A larger decline is projected in Landolfi *et al* (2017), which also considers the atmospheric N_2O increase relative to a fixed preindustrial value. Davidson and Kanter (2014) found an almost 50% increase of total global N_2O emissions in high emission scenarios, while only 22% increase in low emission scenarios when compared to 2005. In this study, we couple terrestrial and oceanic N_2O emissions modules of an Earth system model and assess long term impacts and forcing of atmospheric N_2O concentrations on different future emission scenarios.

2. Methodology

2.1. Model description

The University of Victoria Earth system climate model (UVic ESCM version 2.10), is a global intermediate complexity climate model (Weaver *et al* 2001, Mengis *et al* 2020). It has a three dimensional ocean general circulation represented by the Modular Ocean Model version 2 (MOM2), coupled to a simple atmosphere represented by a simplified moisture-energy balance structure (Fanning and Weaver 1996). The ocean is coupled to a thermodynamic–dynamic sea–ice model (Bitz *et al* 2001).

The ocean module contains ocean biogeochemistry (Keller *et al* 2012, Somes and Oschlies 2015,

Landolfi *et al* 2017). The prognostic global nitrogen budget includes atmospheric N deposition, N_2 fixation, water column denitrification, and benthic denitrification (Somes and Oschlies 2015, Somes *et al* 2016). The oceanic subsurface N_2O production is a function of O_2 consumption with a linear O_2 dependency, including both nitrification and denitrification (Zamora *et al* 2012, Zamora and Oschlies 2014, Landolfi *et al* 2017). In O_2-deficient waters (<4 mmol m^{-3}), denitrification becomes a sink of N_2O in our model, that is consumed at a constant rate. A detailed description of the N_2O module can be found in Landolfi *et al* (2017).

The terrestrial module represents vegetation dynamics and five functional types that interact with each other (Mengis *et al* 2020). As a result of photosynthesis, carbon is captured and allocated to growth and respiration, whereas vegetation provides carbon to the soil in the form of litter fall. The model contains crops and grazing lands that were adapted by aggregating croplands and grazing lands into a single 'crop' type. The crops are represented as a fraction of each grid cell and are assigned to C3 and C4 grasses (Mengis *et al* 2020).

The model has recently been upgraded to include a terrestrial nitrogen and phosphorus cycle. In this variant called UVic ESCM-CNP the terrestrial nitrogen cycle module represents the flow of nitrogen among three organic pools (litter, soil organic matter, and vegetation) and two inorganic pools (NH_4^+ and NO_3^-). Inorganic nitrogen inputs consists of biological nitrogen fixation, atmospheric deposition and agricultural fertilization. A detailed description of the model can be found in De Sisto *et al* (2023).

In the UVic ESCM-CNP (De Sisto *et al* 2023), the wetland module determines anoxic fractions for each soil layer, based on the wetland scheme of Gedney and Cox (2003). Nzotungicimpaye *et al* (2021) implemented the determination of inundated soils and saturated layer fraction in the UVic ESCM. The anoxic fraction, is taken to be the saturated fraction of the soil layer that is shielded from O_2. Denitrification is only allowed to be estimated in soils with anoxic fractions and is calculated as in equation (1):

$$R_{an} = K_{rNO_3} f_t f_m C_s A_f \frac{[NO_3\,(av)]}{[NO_3\,(av)] + K_n}, \qquad (1)$$

where R_{an} is the anaerobic respiration, K_{rNO_3} is the ideal respiration rate via NO_3 reduction, f_t and f_m are temperature and moisture functions, C_s is the concentration of organic carbon, A_f is the anaerobic fraction of the soil layer, K_n is the half-saturation of N-oxides (Li *et al* 2000).

The determination of Wetlands in our model is dependent on prescribed topographic indexes and soil moisture content, corresponding to areas where the formation of wetlands is possible in nature. As in Nzotungicimpaye *et al* (2021) wetlands are represented if they satisfy the following condition:

$$\lambda_{min} \leqslant \lambda \leqslant \lambda_{max}, \qquad (2)$$

where λ_{min} is the lower threshold representing unsaturated conditions, and λ_{max} represents saturated conditions. Wetland areas are sensitive to changes in precipitation and evapotranspiration rates. Globally averaged precipitation increases as a function of warming temperatures. Evapotranspiration also increases with higher temperatures, subject to physiological manipulation by simulated plants.

As N_2O and NO are intermediate products of denitrification and nitrification the complex modelling representation is handled as a 'leaky-pipe' conceptualization of soil-nitrogen processes as in Firestone and Davidson (1989). In this conceptual model N_2O and NO leak out of reactions of one species of nitrogen into another, during nitrification (NH_4 to NO_3) and denitrification (NO_3 to N_2). The size of the holes is determined by the soil processes. In the UVic ESCM version 2.10 the size of the holes controlling the amount of gas that can be leaked is fixed. Using Davidson *et al* (2000) equation the partitioning ratio between NO and N_2O changes based on water filled pore space of the soil layer. The ratio is estimated as in equation (2):

$$\frac{N_2O}{NO} = 10^{2.6 S_U - 1.66}, \qquad (3)$$

where S_U is the waterfilled pore space. Thus, the model produces a total flux of both NO and N_2O for nitrification and denitrification, which is partitioned between the two species based on the above relationship. The NO flux is added to the atmosphere and redeposited as part of the nitrogen deposition flux. The N_2O has a constant lifetime of 100 years. Decayed N_2O is assumed to become part of the atmospheric N_2 pool. The implementation of terrestrial N_2O in the UVic ESCM version 2.10 was shown in De Sisto *et al* (2023).

The new coupled terrestrial–ocean N_2O module is now able to estimate ocean and terrestrial N_2O emissions. A new model modification also allows to represent dynamic N_2O lifetime decrease. In the UVic ESCM version 2.10 only the estimation of ocean N_2O was plausible. This new update introduces the determination of N_2O from terrestrial grids. This modification allows for the accumulation of global atmospheric N_2O concentrations from the most relevant sources of emissions.

2.1.1. Experimental design and forcing data

The CNP version of the UVic ESCM version 2.10 (Mengis *et al* 2020, De Sisto *et al* 2023) was coupled to the ocean N_2O module developed by Landolfi *et al* (2017). The new coupled terrestrial and ocean N_2O modules were used to run all the simulations

in this study. The model was spun up for 6000 years with boundary conditions as outlined in the CMIP6 protocol (Eyring *et al* 2016) and fixed atmospheric N_2O concentration of 270 ppb. Historical N_2O emissions were tuned to match historical observations by adjusting the denitrification N_2O 'leakage' hole size from NO_3 to N_2. Historical temperatures were calibrated using aerosol scaling to match historical observations. Three-dimensional aerosol optical depth can be scaled by a fraction in the UVic ESCM and was used in version 2.10 to calibrate aerosol forcing to fit current values (Mengis *et al* 2020).

Given that N_2O is closely linked to anthropogenic inputs and socioeconomically factors, our simulations project emission using Shared Socioeconomic Pathways (SSPs) to represent different future scenarios (Gidden *et al* 2019). Six SSPs scenarios were run, we included the following: SSP1-1.9, SSP2-4.6, SSP2-4.5, SSP3-7.0, SSP5-3.4-OS and SSP5-8.5 ext. SSP4-3.4 and SSP4-6.0 were excluded from the study due to lack of nitrogen fertilizers inputs for these scenarios. These scenarios are the same used in the Coupled Model Intercomparison Project phase 6 (CMIP6) (Eyring *et al* 2016). Artificial and manure fertilizers data were used in the model simulations. The historical and SPPs fertilizer data were obtained from the publicly available CMIP6 data (Tachirii *et al* 2019). The datasets represent N fertilization from 1850-2100.

We have compared our atmospheric N_2O concentration with the projected by Meinshaussen *et al* (2020). In their study Meinshaussen *et al* (2020) provided atmospheric N_2O concentrations for long-term climate analysis using the reduced-complexity climate–carbon-cycle model MAGICC 7. Meinshaussen *et al* (2020) used Prather *et al* (2012) model to set N_2O assumptions and lifetimes to calibrate MAGICC 7.

A model sensitivity analysis has been carried for key N_2O parameters and forcing data, including nitrogen fertilization, denitrification leaky hole size, and dynamic atmospheric decreasing N_2O lifetime as predicted in Prather *et al* (2015). In the sensitivity analysis N_2O is dynamic. The lifetime reduction was determined by using Meinshaussen *et al* (2020) factor:

$$N_2O_{ltf} = \left(\frac{C^{t}_{N_2O}}{C^{0}_{N_2O}}\right)^{S_{\tau N_2O}}, \quad (4)$$

where N_2O_{ltf} is the N_2O lifetime factor that determines the reduction of N_2O lifetime based on atmospheric N_2O burden, $C^{t}_{N_2O}$ is the N_2O burden per timestep, $C^{0}_{N_2O}$ is the initial N_2O burden, and $S_{\tau N_2O}$ is a sensitivity coefficient. The sensitivity coefficient was set to -0.04 in Meinshaussen *et al* (2020) study. Here, we assume sensitivity coefficient of -2 to assess the model sensitivity, that corresponds roughly to a 20% decrease of N_2O lifetime. This assumption is based on the $-2.1 \pm 1.2\%$ reduction of N_2O lifetime reported by Prather *et al* (2015).

To understand the role of agricultural fields on terrestrial N_2O emissions in the model, we have compared N fertilization map inputs to terrestrial denitrification cover. This approach help to understand the model weakness in regards to agricultural N_2O emissions and sensitivity to N fertilizers.

To assess the response of temperature to N_2O concentrations between our model structure and Meinshaussen *et al* (2020) results, we have prescribed N_2O concentrations using Meinshaussen *et al* (2020) projected atmospheric N_2O into our model N_2O module and compared the resulting temperature response to our UVic ESCM- CNP with N_2O dynamics. As temperature response varies depending on model climate sensitivity we have set three different model variants tuned to have Equilibrium Climate Sensitivities (ECSs) per doubling of CO_2 of 2.0 °C, 4.5 °C to represent the 'likely bounds' (IPCC 2021), as well as using the emergent climate sensitivity of the model (3.4 °C) as the central estimate. The climate sensitivity was tuned using a method designed by Zickfeld *et al* (2009) to alter climate sensitivity in the UVic ESCM by altering the flow of long-wave radiation back to space. Furthermore, the model sensitivity variants serve to assess the impact of climate sensitivity on our model N_2O emissions and hence, atmospheric N_2O concentrations.

3. Results and discussion

3.1. Model sensitivity

The sensitivity simulations shows that the model is highly sensitive to the leaky hole parameter that determines the release of N_2O from denitrification. A change of $\pm 20\%$ of hole size resulted in a corresponding $\pm 5\%$ atmospheric N_2O concentration (table 1). A decline in atmospheric N_2O lifetime (-20%) resulted in a reduction of 3% of atmospheric N_2O concentration. The change in N fertilization shows a N_2O concentration change of $\pm 1\%$ for a corresponding $\pm 20\%$ N input. Finally, atmospheric N_2O concentration from different equilibrium climate sensitivities variants of the models (ECS 2, 3.4 °C and 4.5 °C) did not show a large difference between lower a high climate sensitivities as shown in table 1 and figure 7.

As shown in table 1 the main driver of N_2O atmospheric concentration changes is the anaerobic fraction in soil. In the UVic ESCM version 2.10, these fractions are determined by saturation of soil layers. In the model the accuracy of saturated soil layers is likely impacted by the lack of dedicated agricultural dynamics. Figure 1 shows maps representing N fertilizers and denitrification in simulations, showing regions where denitrification is not utilizing the fertilizer input. Thus, declining the model sensitivity for fertilizer changes.

Table 1. Mean SSPs atmospheric N_2O concentration percentage change to modified N fertilization, denitrification leaky hole, atmospheric N_2O lifetime (here lifetime is a dynamic value instead of a parameter, that reduces the lifetime by 20% by 2100) and ECS. The N_2O lifetime was only decreased as it is what is projected in literature (Prather *et al* 2015). The temperature sensitivities are compared to the base 3.4 ECS of the UVic ESCM version 2.10.

Input-Parameter-Variable	−20% change	+20% change	ECS2.0	ECS4.5
N fertilization	−1%	+1%	—	—
Denitrification leaky hole	−5%	+5%	—	—
N_2O lifetime	−3%	—	—	—
Temperature	—	—	−0.3%	+0.5%

3.2. Historical and projected N_2O atmospheric concentrations and emissions

The coupled terrestrial and ocean N_2O dynamics from De Sisto *et al* (2023) and Landolfi *et al* (2017) were tuned to match historical atmospheric N_2O concentrations. Figure 2 shows the N_2O concentration simulated with the UVic ESCM compared to Machida *et al* (2015), Lan *et al* (2023)and Prinn *et al* (2023). The model outputs follow observations closely. The preindustrial atmospheric N_2O concentration captures the ice cores observations from Machida *et al* (2015) with high fidelity. After 1945 we observed a divergence between our increase of N_2O concentrations and atmospheric measurements. This divergence is likely a consequence of a simplified representation of agriculture, where in both natural and agricultural fractions of grid cells feed into the same subsurface soil column in our model. Despite this limitation the model represents fairly well the historical trends and magnitudes. For the year 2023 we estimate a N_2O concentration of 335 ppb, close to the NOAA (Lan *et al* 2023) measurement of 336 ppb locating our results close to historical atmospheric N_2O concentrations. From 2000 to 2005 we simulated an atmospheric N_2O growth rate between 0.86 and 0.89 ppb yr^{-1} similar to the value of 0.73 reported by NOAA (Hall *et al* 2007). However, our model lacks the annual variability of atmospheric growth rate shown in Tian *et al* (2020). This lack of variability can be attributed to the lack of internal variability in the UVic ESCM and a constant N_2O decay prescribed in the UVic ESCM rather than a dynamic change as shown in Prather *et al* (2023). Prather *et al* (2023) simulated a reduction of N_2O lifetime over the period of 2005–2100 that indicates that the accumulation of N_2O could be slowed down as N_2O is reduced more rapidly photochemically from the atmosphere. The lack of decay dynamics in our model can lead to overestimation in our simulations results by the end of the 21st century.

3.2.1. Oceanic N_2O emissions

Both terrestrial and oceanic N_2O modules simulate fluxes within the range of uncertainty of other studies. The ocean N_2O is similar to Landolfi *et al* (2017) oceanic N_2O emissions. Our simulations represents a decline in ocean N_2O emissions from 3.6 to 3.0 Tg N yr^{-1} from 1850 to 2020 and to 2.7 [2.6–2.8] Tg N yr^{-1} by 2100 (figure 3). The historical results are consistent with the IPCC range of 1.8–9.45 Tg N yr^{-1} and other studies such as Martinez-Rey *et al* (2015) estimating a range of 3.71–4.03 Tg N yr^{-1} (2005), Landolfi *et al* (2017) with a value of around 3.2 Tg N yr^{-1} and Yang *et al* (2020) with a value of 4.2 ± 1.0 TgN yr^{-1}. For the end of the 21st century, we simulate a reduction of 0.9 TgN yr^{-1} [0.8–1 TgN yr^{-1}] . This decline is also shown by Landolfi *et al* (2017) where by 2100 ocean N_2O emissions decline by around 1.1 TgN yr^{-1} for most simulations from 1850 to 2100 mainly due to reduced temperature-dependent surface solubility and transport to greater depths. Furthermore, Martinez-Rey *et al* (2015) reports a decline between 0.15–0.49 TgN yr^{-1} from 2005 to 2100. These values are comparable to our 0.3 TgN yr^{-1} [0.2–0.4 TgN yr^{-1}] decline simulated from 2020 to 2100.

As in Landolfi *et al* (2017), the warming-induced mean reduction of the mixed layer depth of −5% [−9%–1%] from 1850 to 2100, increases the nutrient limitation by declining the supply of nutrients to primary producers in tropical latitudes. The reduced supply increases nitrogen and phosphorus limitation to phytoplankton and hence, reduces ocean productivity. On the other hand, the ocean oxygen concentration declines overall from 197 to 188 mmol m^{-3} [186–190] between 1850–2100. Consequently, this leads to an increase in the size of oxygen deficient zones where water column denitrification and N_2O consumption occur. This increase is overcompensated by the decline in export production and consequently, the decline of N_2O production in water with high oxygen concentrations via nitrification. However, in the high emissions scenario with highest levels of oxygen decline, marine N_2O production reaches an inflection point where marine N_2O emissions begin increasing before the year 2100. This indicates that severe ocean oxygen decline can eventually drive increased ocean N_2O emissions on long time scales. The reduction of fluxes reduces the growth rate of N_2O concentration in the atmosphere, but it is rapidly overcome by the terrestrial increase of N_2O due to fertilizer inputs.

3.2.2. Terrestrial N_2O emissions

The terrestrial N_2O emissions in 2020 was estimated to be 11 TgN yr yr^{-1}. This value is within the range of 8–12 TgN yr^{-1} reported in Tian *et al*

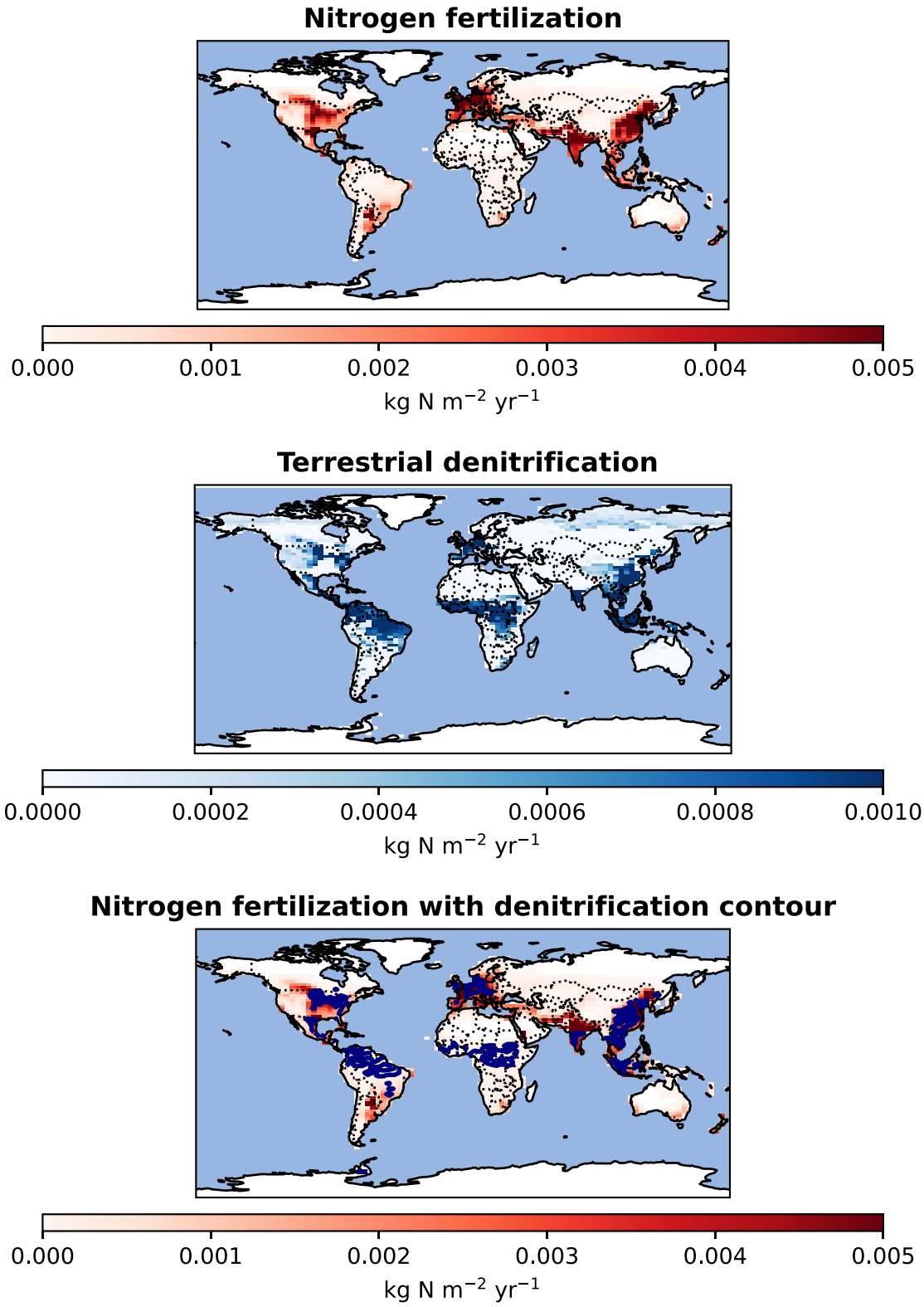

Figure 1. N fertilization for 2020, terrestrial denitrification and N fertilization compared to denitrification coverage. In the bottom plot, red regions outside blue contour represent locations where denitrification is not estimated.

(2020) and Crippa *et al* (2021). In preindustrial years, our fluxes underestimate the value of around 6 TgN yr^{-1} reported in Tian *et al* (2020) by 2 TgN yr^{-1}. However, as shown in figure 2, this magnitude of emissions seems to represent the preindustrial atmospheric N_2O concentrations along with the marine N_2O emissions with high fidelity. After 1945 the increasing nitrogen fertilizers led to the rise of N_2O

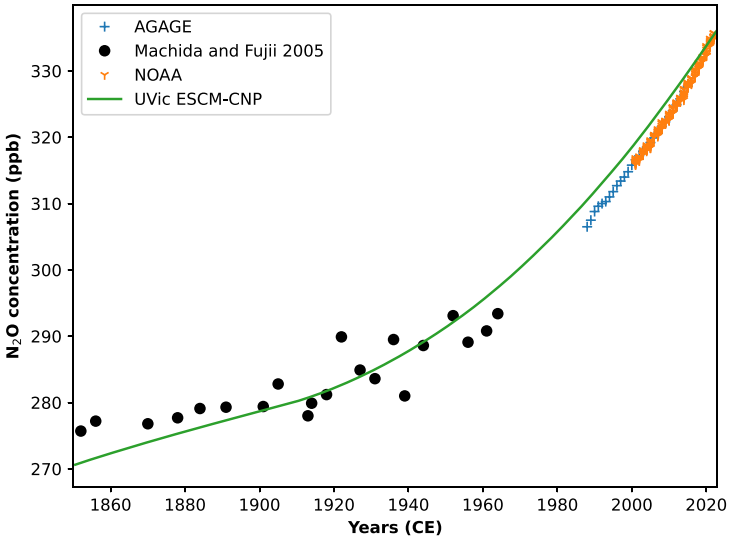

Figure 2. Historical atmospheric N_2O concentrations, estimated using a terrestrial and ocean N_2O modules in the UVic ESCM version 2.10. Machida *et al* (2015) measured the concentration of N_2O from Antarctic ice cores, the N_2O measurement covers 1735–1965. AGAGE (Prinn *et al* 2023) and NOAA (Lan *et al* 2023) show monthly atmospheric N_2O measurements.

emissions and are a key factor for the rise of N_2O concentrations in the atmosphere. Our model shows a good fit with concentration measurements, as shown in figure 2. With decreasing ocean emission rates, the terrestrial system is primarily responsible for the future rise of N_2O concentrations. We found a historical rise of 6 TgN yr^{-1} between 1850 and 2020. The total oceanic and terrestrial N_2O emissions for the year 2020 was simulated to be 13 TgN yr^{-1}. This value falls within the range of uncertainty presented by the IPCC AR6 report and Tian *et al* (2020).

Our model estimates different terrestrial N_2O emissions for six SSP simulations. There are three main reasons behind this difference: (1) the change of temperature that determines the rate of biological processes, (2) the rate of N fertilizers input, projected differently based on each scenario narrative, and (3) the differences in model soil saturated fraction for each SSP scenario that determines the anaerobic cover in our model. Among these, the representation of soil saturated cover area differences is by far the most important (figure 1) and as shown in our sensitivity analysis. For the year 2050 our model simulates a mean terrestrial N_2O emission of 13 TgN yr^{-1} [12–14 TgN yr^{-1}]. By 2100 we simulated a mean terrestrial N_2O emission of 14 TgN yr^{-1} [12–16 TgN yr^{-1}] (figure 4). The differences between terrestrial N_2O emissions among SSPs simulations coincide with the rate of increase or decrease of wetlands areas and consequently the anaerobic fractions in soils estimated by the model. In the UVic ESCM-CNP the anaerobic fraction is estimated from grid inundations given by a wetland scheme. The wetland cover was expanded in model simulations from 1.9×10^6 km^{-2} in 1850 to 2.2×10^6, 2.4×10^6, 2.6×10^6, 2.8×10^6, 3.2×10^6 and 3.4×10^6 km^{-2} by 2100 in SSP1-1.9, SSP1-2.6, SSP2-4.5, SSP3-7.0, SSP5-3.4 and SSP5-8.5 correspondingly. These terrestrial aquatic interfaces simulated by the model peak from around 2030 in low-emission scenarios and continue to increase in high-emission scenarios. This feedback gives a clear hint of a possible reduction of N_2O increase in natural systems in the future due to the reductions of terrestrial-aquatic interfaces. As our model does not have a dedicated agricultural subsurface module, the reduction of N_2O emission is likely overestimated as agricultural irrigation is not accounted for in this simulation and hence, the anaerobic fractions estimated here are uncertain. However, it is possible that the anaerobic respiration in natural systems will reduce the rate of increase of N_2O emissions as aquatic systems dry.

The observed trend shows an increase of terrestrial N_2O emissions from tropical and sub-tropical regions. In low emission SSPs (SSP1-1.9 and SSP1-2.6) the increase in emissions is especially located in tropical regions with hotpots in non-desert regions while in high challenged scenarios, this increase is spread towards high latitudes and clearly shows an increase in Eastern Europe and North America (figure 5). This increase is mainly due to how nitrogen fertilizers will develop in different climate scenarios. This is in line with Harris *et al* (2022), where N_2O increase with agricultural demand and is predicted to mainly be located in tropical regions as N_2O mitigation controls would be in place in developed countries. Harris *et al* (2022) identified that non-desert tropical regions, especially sub-Saharan Africa,

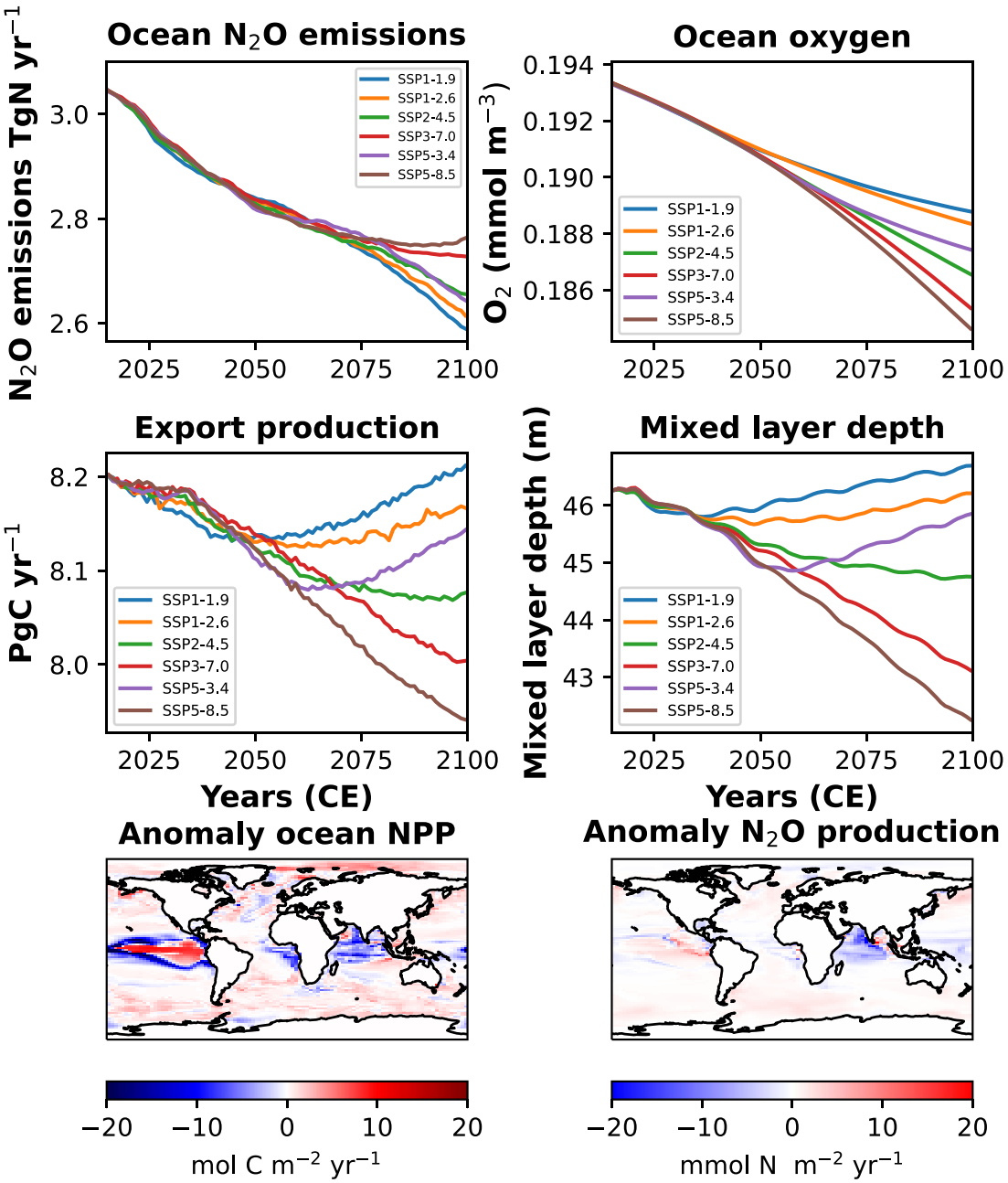

Figure 3. Ocean N_2O relevant variables: ocean N_2O emissions, oxygen concentration, NPP and mixed layer depth for each SSPs simulations. The final two maps show the mean ocean NPP and ocean N_2O production from 2090 to 2100 relative to 1850–1860 in SSPs simulations.

southern India, China, and south east Asia would have the largest increase, agreeing with what is shown in our results.

3.2.3. Predicted N_2O concentration for 2100

Terrestrial N_2O emissions are the most important source of N_2O to atmospheric concentrations. Given that atmospheric temperature, N fertilizers, and anaerobic fractions vary among SSP narratives our model simulated different atmospheric N_2O concentrations by the 21st century (figure 6). Our results are closer in value than the projected by Meinshaussen *et al* (2020), where in year 2100 SSP1-1.9N_2O concentration is projected to have a value of 351 ppb and SSP3-7.0N_2O concentration of 421 ppb, representing the lowest and the highest concentrations. For 2100 our model projects SSP1-1.9N_2O concentration of 401 ppb and SSP2-4.5N_2O concentration of 418 ppb representing the lowest and the highest concentrations. These results show that the difference between the low to the high range of atmospheric N_2O concentration is 67 ppb in Meinshaussen *et al* (2020) and 17 ppb for the UVic ESCM-CNP simulations. Furthermore, our lowest estimate for future N_2O concentration by 2100 is higher than the value projected by Meinshaussen *et al* (2020). This lowest estimate corresponds to low-emission SSPs scenarios.

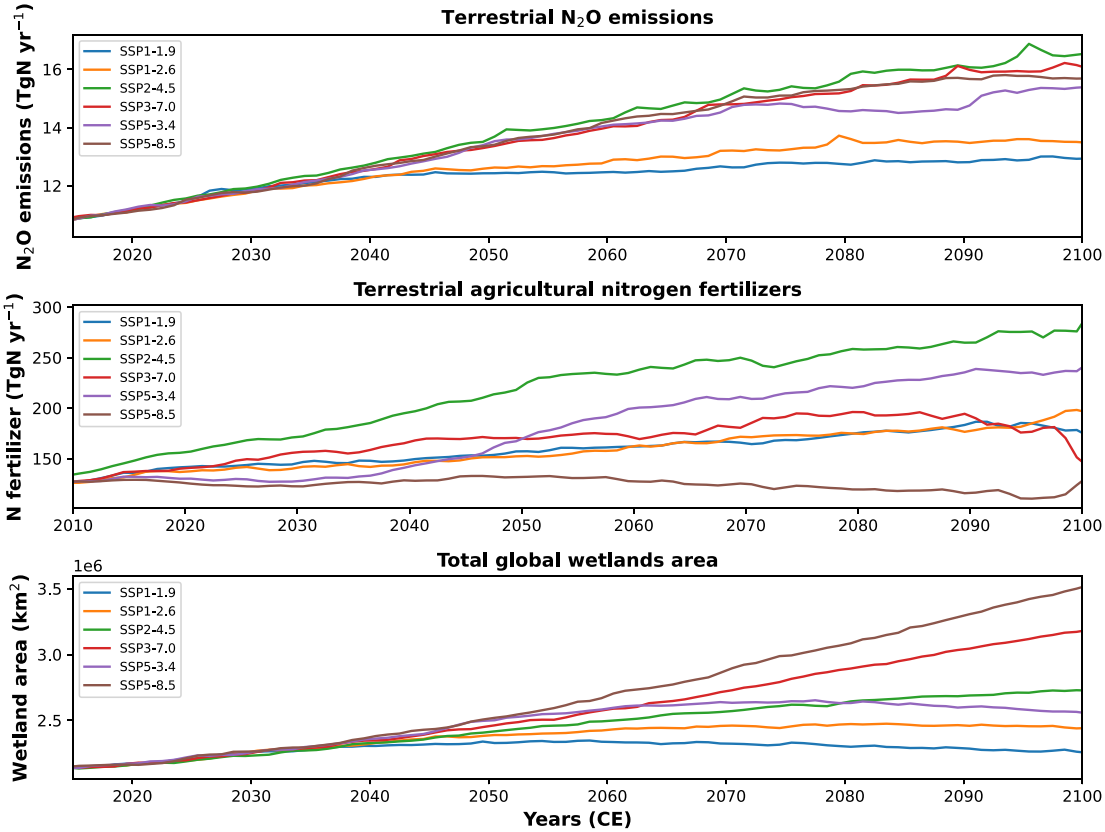

Figure 4. Terrestrial N_2O emissions, N_2 emissions and wetland area for each SSPs simulations from 2010 to 2100.

These results and differences reflect important dynamics in N_2O systems and uncertainties of Earth system models when simulating N_2O emissions. The first observable dynamic is that N_2O concentration will keep rising until it peaks beyond the 21st-century timeline, even in low emission scenarios where terrestrial N_2O emission peaks around the year 2030. The second dynamic in our model corresponds to how saturated soils are simulated. Saturated soils layers provide anoxic conditions needed to produce N_2O, and thus how saturated soils are represented has a strong impact on simulated N_2O production on land. This means that the representation of anaerobic soil dynamics in Earth system models is of utmost importance for accurately estimating N_2O concentration in future simulations. On the other hand, the high sensitivity to SSPs scenarios in Meinshaussen *et al* (2020) might correspond to idealistic assumptions for atmospheric N_2O concentration projection that would require a substantial decrease of terrestrial N_2O emissions in our model.

The equation that estimates N_2O emission input used in Meinshaussen *et al* (2020) is controlled by the emissions of the specific pollutant per country, the absence of emission control measures, the reduction efficiency, and the actual implementation rate of the considered abatement. Hence, the variables that determine the N_2O emission in Meinshaussen *et al* (2020) account for mitigation efforts per SSPs. Furthermore, Meinshaussen *et al* (2020) account for dynamic changes of N_2O lifetimes. Both N_2O mitigations and dynamic lifetime are not accounted for in our modelling structure. Consequently, the reduction of atmospheric N_2O concentration would likely come from intensive management practices to reduce agricultural N_2O emissions and a slower increase of atmospheric N_2O concentration due to the projected decrease of N_2O lifetime. Our sensitivity analysis have shown that for a 20% decrease of N_2O lifetime, atmospheric N_2O concentration estimated is 3% lower. This partially explain the differences in our estimations with Meinshaussen *et al* (2020). However, a large portion of unexplained differences likely comes from agricultural dynamics lacking by the UVic ESCM version 2.10, especially those regarding irrigation and denitrification.

The difference between our simulated atmospheric N_2O with a dynamic N_2O structure and simulations with Meinshaussen *et al* (2020) N_2O concentrations forcing resulted in contrasting global temperatures among the SSPs scenarios (figure 8). We report a range of −0.02 °C to 0.09 °C difference between the dynamic atmospheric N_2O simulated and the prescribed simulations with Meinshaussen *et al* (2020) data. In scenarios where our atmospheric N_2O concentrations were close in value to Meinshaussen *et al* (2020) dataset, the temperature difference between our model and Meinshaussen *et al* (2020) values was

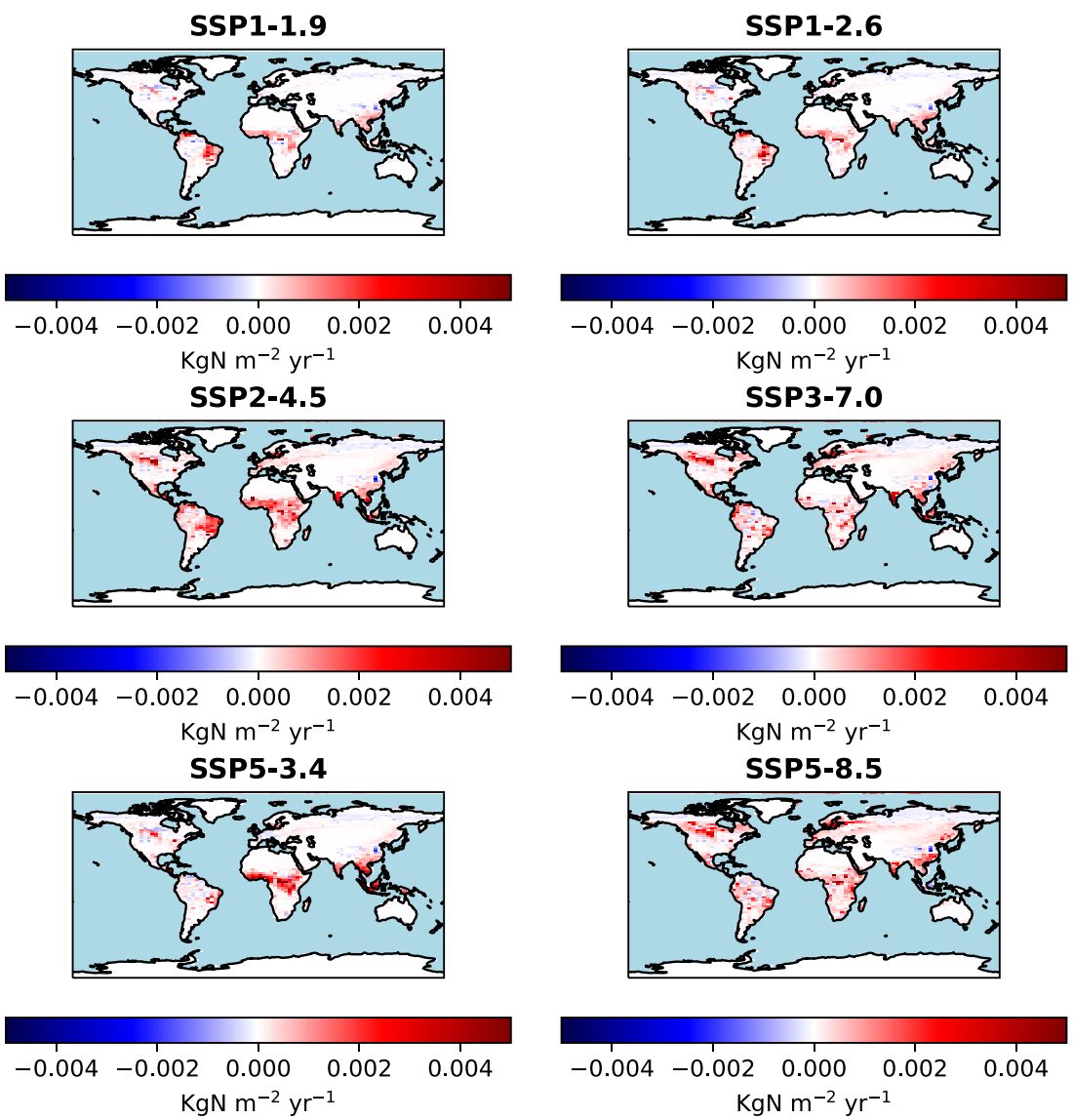

Figure 5. Terrestrial N_2O flux to atmosphere difference between year 2020 and 2100 for SSPs simulations.

the lowest. Conversely, where large differences of N_2O concentrations were observed, the temperature difference was larger as a result. Our simulations for low emission SSP scenarios have higher atmospheric N_2O concentration than Meinshaussen *et al* (2020), while our high emission scenarios simulations tend to have lower N_2O concentrations than Meinshaussen *et al* (2020). The temperature 1.5 °C and 2 °C targets were shown to be affected by the concentration of atmospheric N_2O. The dynamic structure decreased the time for our simulations to reach 1.5 °C and 2 °C among the SSP scenarios by one to two years.

Our results suggest that atmospheric N_2O concentrations seem to be relatively insensitive to mitigation efforts among the SSP simulations. The low sensitivity can be in part due to a low sensitivity to N fertilizer as shown in our sensitivity analysis. Nonetheless, Meinshaussen *et al* (2020) results could overestimate the effect of SSPs inputs of N_2O by using over-optimistic mitigation in the approach. For the UVic ESCM version 2.10 structure, there is a clear need for a more sophisticated agricultural model structure. Under idealistic scenarios, the mitigation of N_2O should be targeted directly with proper management schemes. Future coupled N_2O models should take into account N_2O management practices to avoid this lack of sensitivity. However, global estimates of mitigation efficiency and deployment feasibility needs to be assessed before such mitigation could be part of N_2O dynamic models.

3.3. Model uncertainties

There are many model uncertainties around the estimation of N_2O emission and the atmospheric chemistry of N_2O. In the ocean, N_2O production representation is sensitive to estimations of productivity,

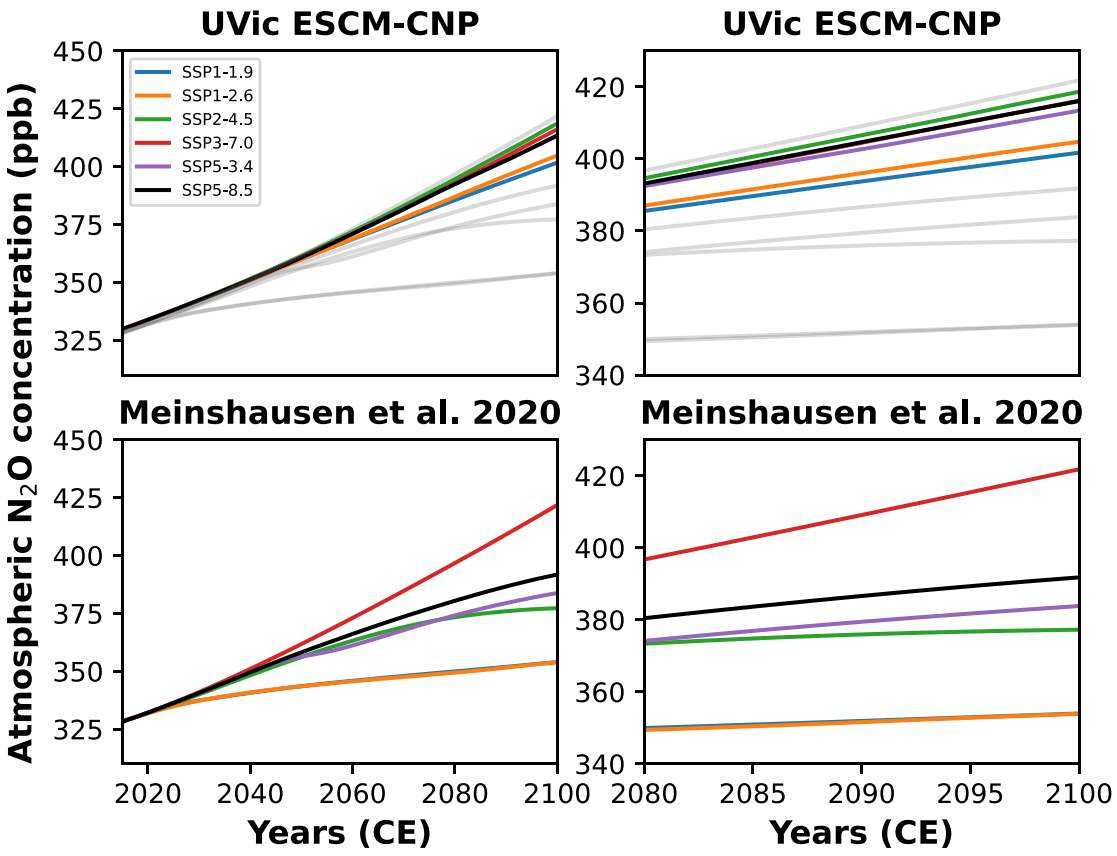

Figure 6. Top left: atmospheric N_2O projection from year 2015 until 2100 for each SSP simulation in the UVic ESCM-CNP. Top right: atmospheric N_2O projection from year 2080 until 2100 for each SSP simulation in the UVic ESCM-CNP. The background grey lines in the top panels represent Meinshaussen *et al* (2020) projections. Bottom left: atmospheric N_2O projection from year 2015 until 2100 projected by Meinshaussen *et al* (2020). Bottom right: atmospheric N_2O projection from year 2080 until 2100 projected by Meinshaussen *et al* (2020).

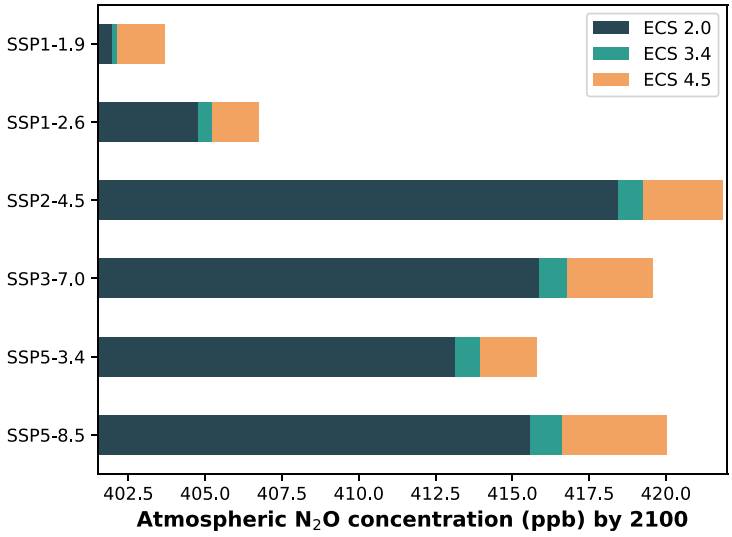

Figure 7. Atmospheric N_2O concentration sensitivity to equilibrium climate sensitivity (ECS). Three sensitivities were simulated for each SSP scenario: ECS 2, 3.4 °C and 4.5 °C.

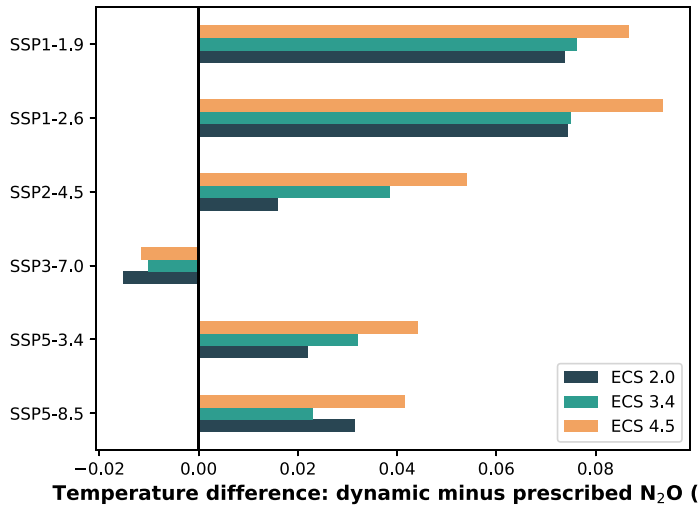

Figure 8. N_2O forcing effect on atmospheric temperature in a dynamic (current UVic ESCM-CNP simulations) and prescribed (Meinshaussen *et al* 2020) N_2O concentrations projections averaged over year 2080 to 2100. Lower temperature differences reflect scenarios were the UVic ESCM-CNP and Meinshaussen *et al* (2020) N_2O concentrations are more similar. ECS is Equilibrium Climate Sensitivity.

oxygen concentration and oxygen minimum zones. Consequently, the marine biogeochemical uncertainties influencing these variables are crucial for a more accurate estimation of marine N_2O emissions. On land, the representation of anaerobic dynamics limits the capacity of the utilization of nitrogen agricultural fertilizers. In our model, the lack of agricultural dynamics constitutes a substantial source of uncertainty. In terms of N_2O land emissions, the lack of agricultural land lowers the accuracy of denitrification cover representation. This decrease of accuracy as shown in the sensitivity analysis can affect the sensitivity of the model to SSPs scenarios as it reduces how sensible the model is to changes in N fertilizers. Furthermore, the lack of N_2O mitigation is a source of uncertainty in future N_2O projections as our simulations show low sensitivity to the mitigation efforts represented in the SSPs scenarios. Among the possible N_2O mitigation efforts that could be included are slow-release fertilizers, nitrification inhibitors, appropriate crop rotations and schemes, tillage and irrigation practices and the use of biochar and lime (Hassan *et al* 2022). The plausibility of the global application of terrestrial N_2O mitigation strategies needs to be addressed in future studies to assess the effectiveness and, consequently, reassess if these mitigation efforts can be realistically deployed and added to the SSP mitigation efforts for N_2O projections. Finally, our model lacks dynamic N_2O atmospheric chemistry dynamics. Hence, N_2O lifetimes remain constant in our simulation, underestimating the sensitivity of atmospheric N_2O accumulation to changes if N_2O lifetimes.

4. Conclusions

To our knowledge, this study is the first to successfully couple an ocean and terrestrial N_2O modules and the resulting model to project atmospheric N_2O concentrations to the end of the 21st century. In the ocean, we project a decline of N_2O emissions from 3.7 to around 2.6 TgN yr^{-1} by 2100. On land, we simulated N_2O emission from 4 TgN yr^{-1} in preindustrial times to between 12–16 TgN yr^{-1} depending on SSP scenario in the year 2100. In the atmosphere, we project an atmospheric N_2O concentration between 401 and 418 ppb in six SSPs scenarios. We report at least 49 ppb more atmospheric N_2O concentrations than Meinshaussen *et al* (2020) by 2100 corresponding to low-emission scenarios projections. Our results suggest that atmospheric N_2O concentrations seem to be relatively insensitive to mitigation efforts among the SSP simulations. The low sensitivity can be in part due to a low sensitivity to N fertilizer as shown in our sensitivity analysis. Nonetheless, Meinshaussen *et al* (2020) results could overestimate the effect of SSPs inputs of N_2O by using over-optimistic mitigation in the approach. Improving the representations of agricultural model dynamics and cover, as well as, anaerobic soil representation in croplands should be prioritized to improve the accuracy of terrestrial N_2O emissions and atmospheric N_2O concentration representation in simulations. For the UVic ESCM version 2.10 structure, there is a clear need for a more sophisticated agricultural model structure. Under idealistic scenarios, the mitigation of N_2O should be targeted directly with proper management schemes. However,

global estimates of mitigation efficiency and deployment feasibility needs to be assessed before such mitigation could be part of N_2O dynamic models. Overall we assess that N_2O will remain an important greenhouse gas for the remainder of the 21st century, with a potential for larger impacts further into the future.

Data availability statement

The data that support the findings of this study are openly available at the following URL/DOI: https://doi.org/10.5683/SP3/GXYZKU.

Funding

M D S and A H M were supported by the Natural Science and Engineering Research Council of Canada Discovery Grant program and Compute Canada (now the Digital Research Alliance of Canada). C S was supported by the Deutsche Forschungsgemeinschaft (Project No. 445549720).

ORCID iDs

M De Sisto https://orcid.org/0009-0001-3478-3555
C Somes https://orcid.org/0000-0003-2635-7617
A H MacDougall https://orcid.org/0000-0003-1094-6783

References

Arévalo-Martínez D L, Kock A, Löscher C R, Schmitz R A and Bange H W 2015 Massive nitrous oxide emissions from the tropical South Pacific Ocean *Nat. Geosci.* **8** 530–3

Battaglia G and Joos F 2018 Marine N_2O emissions from nitrification and denitrificationconstrained by modern observations and projected in multimillennial global warming simulations *Glob. Biogeochem. Cycles* **32** 92–121

Bitz C M, Holland M M, Weaver A J and Eby M 2001 Simulating the ice-thickness distribution in a coupled *J. Geophys. Res. Lett.* **106** 2441–63

Bopp L *et al* 2013 Multiple stressors of ocean ecosystems in the 21st century: projections with CMIP5 models *Biogeosciences* **10** 6225–45

Buitenhuis E T, Suntharalingam P and Le Quéré C 2018 Constraints on global oceanic emissions of N_2O from observations and models *Biogeosciences* **15** 2161–75

Canadell J G *et al* 2021 Global carbon and other biogeochemical cycles and feedbacks *Climate Change 2021: The Physical Science Basis. Contribution of Working Group I to the Sixth Assessment Report of the Intergovernmental Panel on Climate Change* ed V Masson-Delmotte *et al* (Cambridge University Press) pp 673–816

Caranto J and Lancaster K 2017 Nitric oxide is an obligate bacterial nitrification intermediate produced by hydroxylamine oxidoreductase *Proc. Natl Acad. Sci.* **114** 201704504

Carreira C, Mestre O, Nunes R F, Moura I and Pauleta S R 2018 Genomic organization, gene expression and activity profile of Marinobacter hydrocarbonoclasticus denitrification enzymes *PeerJ* **6** e5603

Chen J and Strous M 2012 Denitrification and aerobic respiration, hybrid electron transport chains and co-evolution *Biochim. Biophys. Acta* **1827** 136–44

Crippa M, Guizzardi D, Muntean M, Schaaf E, Lo Vullo E, Solazzo E, Monforti-Ferrario F, Olivier J and Vignati E 2021 *EDGAR v6.0 Greenhouse Gas Emissions* (European Commission, Joint Research Centre (JRC)) (available at: http://data.europa.eu/89h/97a67d67-c62e-4826-b873-9d972c4f670b)

Davidson E and Kanter D 2014 Inventories and scenarios of nitrous oxide emissions *Environ. Res. Lett.* **9** 105012

Davidson E, Keller M, Erickson H, Verchot L and Veldkamp E 2000 Testing a conceptual model of soil emissions of nitrous and nitric oxides: using two functions based on soil nitrogen availability and soil water content, the hole-in-the-pipe model characterizes a large fraction of the observed variation of nitric oxide and nitrous oxide emissions from soils *AIBS Bull.* **50** 667–80

De Sisto M L, MacDougall A H, Mengis N and Antoniello S 2023 Modelling the terrestrial nitrogen and phosphorus cycle in the UVic ESCM *Geosci. Model Dev.* **16** 4113–36

Eyring V, Bony S, Meehl G A, Senior C A, Stevens B, Stouffer R J and Taylor K E 2016 Overview of the Coupled Model Intercomparison Project Phase 6 (CMIP6) experimental design and organization *Geosci. Model Dev.* **9** 1937–58

Fanning A F and Weaver A J 1996 An atmospheric energy-moisture balance model: climatology, interpentadal climate change and coupling to an ocean general circulation model *J. Geophys. Res.* **101** 111–5

Firestone M and Davidson E 1989 *Exchange of Trace Gases Between Terrestrial Ecosystems and the Atmosphere* vol 47 (Wiley) pp 7–21

Fowler D *et al* 2013 The global nitrogen cycle in the twenty-first century *Phil. Trans. R. Soc.* B **368** 20130164

Gedney N and Cox P 2003 The sensitivity of global climate model simulations to the representation of soil moisture heterogeneity *J. Hydrometeorol.* **4** 1265–75

Gidden M J *et al* 2019 Global emissions pathways under different socioeconomic scenarios for use in CMIP6: a dataset of harmonized emissions trajectories through the end of the century *Geosci. Model Dev.* **12** 1443–75

Groffman P M 2012 Terrestrial denitrification: challenges and opportunities *Ecol. Process.* **1** 11

Guilhen J, Al B, Ahmad S, Sabine P, Marie J, Abril G, Moreira-Turcq P and Sánchez Pérez J 2020 Denitrification, carbon and nitrogen emissions over the Amazonian wetlands *Biogeosciences* **17** 4297–311

Hall B D, Dutton G S and Elkins J W 2007 The NOAA nitrous oxide standard scale for atmospheric observations *J. Geophys. Res.* **112** D09305

Harris E, Yu L and Wang Y P *et al* 2022 Warming and redistribution of nitrogen inputs drive an increase in terrestrial nitrous oxide emission factor *Nat. Commun.* **13** 4310

Hassan M U *et al* 2022 Management strategies to mitigate N_2O emissions in agriculture *Life* **12** 439

IPCC 2022 Climate change 2022 impacts, adaptation and vulnerability *Contribution of Working Group II to the Sixth Assessment Report of the Intergovernmental Panel on Climate Change* ed H-O Pörtner *et al* (Cambridge University Press) p 3056

IPCC 2021 Summary for policymakers *Climate Change 2021: The Physical Science Basis. Contribution of Working Group I to the Sixth Assessment Report of the Intergovernmental Panel on Climate Change* ed V Masson-Delmotte *et al* (Cambridge University Press)

Keller D P, Oschlies A and Eby M 2012 A new marine ecosystem model for the University of Victoria Earth system climate model *Geosci. Model Dev.* **5** 1195–220

Lan X, Thoning K W and Dlugokencky E J 2023 Trends in globally-averaged CH_4, N_2O, and SF_6 determined from NOAA Global Monitoring Laboratory measurements. Version 2023-07 (https://doi.org/10.15138/P8XG-AA10)

Landolfi A, Somes C J, Koeve W, Zamora L M and Oschlies A 2017 Oceanic nitrogen cycling and N2 flux perturbations in the Anthropocene *Glob. Biogeochem. Cycles* **31** 1236–55

Li C, Aber J, Stange F, Butterbach-Bahl K and Papen H 2000 A process-oriented model of N_2O and NO emissions from forest soils: 1. Model development *J. Geophys. Res.: Atmos.* **105** 4369–84

Lu C and Tian H 2017 Global nitrogen and phosphorus fertilizer use for agriculture production in the past half century: shifted hot spots and nutrient imbalance *Earth Syst. Sci. Data* **9** 181–92

Machida T, Nakazawa T, Fujii Y, Aoki S and Watanabe O 1995 Increase in the atmospheric nitrous oxide concentration during the last 250 years *Geophys. Res. Lett.* **22** 2921–4

Manizza M, Keeling R F and Nevison C D 2012 On the processes controlling the seasonal cycles of the air–sea fluxes of O_2 and N_2O: a modelling study *Tellus* B **64** 18429

Martinez-Rey J, Bopp L, Gehlen M, Tagliabue A and Gruber M 2015 Projections of oceanic N_2O emissions in the 21st century using the IPSL Earth system model *Biogeosciences* **12** 4133–48

Meinshausen M *et al* 2020 The shared socio-economic pathway (SSP) greenhouse gas concentrations and their extensions to 2500 *Geosci. Model Dev.* **13** 3571–605

Mengis N *et al* 2020 Evaluation of the University of Victoria Earth system climate model version 2.10 (UVic ESCM 2.10) *Geosci. Model Dev.* **13** 4183–204

Montzka S, Dlugokencky E and Butler J 2011 Non-CO2 greenhouse gases and climate change *Nature* **476** 43–50

Nishida S, Takahashi K, Matsumi Y, Taniguchi N and Hayashida S 2004 Formation of O(3P) atoms in the photolysis of N_2O at 193 nm and O(3P) + N_2O product channel in the reaction of O(1D) + N_2O *J. Phys. Chem.* **108** 2451–6

Norton J and Ouyang Y 2019 Controls and adaptive management of nitrification in agricultural soils *Front. Microbiol.* **10** 1931

Nzotungicimpaye C M, Zickfeld K, Macdougall A H, Melton J, Treat C, Eby M and Lesack L 2021 WETMETH 1.0: a new wetland methane model for implementation in Earth system models *Geosci. Model Dev.* **14** 6215–40

Prather M J, Holmes C D and Hsu J 2012 Reactive greenhouse gas scenarios: systematic exploration of uncertainties and the role of atmospheric chemistry *Geophys. Res. Lett.* **39** L09803

Prather M *et al* 2015 Measuring and modeling the lifetime of nitrous oxide including its variability: nitrous oxide and its changing lifetime *J. Geophys. Res.: Atmos.* **120** 2015JD023267

Prather M, Froidevaux L and Livesey N J 2023 Observed changes in stratospheric circulation: decreasing lifetime of N_2O, 2005–2021 *Atmos. Chem. Phys.* **23** 843–9

Prinn R *et al* 2018 History of chemically and radiatively important atmospheric gases from the Advanced Global Atmospheric Gases Experiment (AGAGE) *ESS-DIVE Repository. Dataset* (Carbon Dioxide Information Analysis Center (CDIAC), Oak Ridge National Laboratory (ORNL) (https://doi.org/10.3334/CDIAC/ATG.DB1001) (Accessed 25 July 2023)

Saud S, Wang D and Fahad S 2022 Improved nitrogen use efficiency and greenhouse gas emissions in agricultural soils as producers of biological nitrification inhibitors *Front. Plant Sci.* **13** 854195

Scheer C, Fuchs K, Pelster D and Butterbach-Bahl K 2020 Estimating global terrestrial denitrification from measured N_2O:(N_2O + N_2) product ratios *Curr. Opin. Environ. Sustain.* **47** 72–80

Somes C J, Landolfi A, Koeve W and Oschlies A 2016 Limited impact of atmospheric nitrogen deposition on marine productivity due to biogeochemical feedbacks in a global ocean model *Geophys. Res. Lett.* **43** 4500–9

Somes C J and Oschlies A 2015 On the influence of non-Redfield dissolved organic nutrient dynamics on the spatial distribution of N_2 fixation and the size of the marine fixed nitrogen inventory *Glob. Biogeochem. Cycles* **29** 973–93

Steinacher M *et al* 2010 Projected 21st century decrease in marine productivity: a multi-model analysis *Biogeosciences* **7** 979–1005

Suntharalingam P, Buitenhuis E, Le Quéré C, Dentener F, Nevison C, Butler J H, Bange H W and Forster G 2012 Quantifying the impact of anthropogenic nitrogen deposition on oceanic nitrous oxide *Geophys. Res. Lett.* **39** L07605

Tachiiri K *et al* 2019 MIROC MIROC-ES2L model output prepared for CMIP6 ScenarioMIP ssp585. Version YYYYMMDD[1] (Earth System Grid Federation) (https://doi.org/10.22033/ESGF/CMIP6.5770)

Tian H *et al* 2016 The terrestrial biosphere as a net source of greenhouse gases to the atmosphere *Nature* **531** 225–8

Tian H *et al* 2020 A comprehensive quantification of global nitrous oxide sources and sinks *Nature* **586** 248–56

Weaver A J *et al* 2001 The UVic Earth system climate model: model description, climatology and applications to past, present and future climates *Atmos. Ocean* **39** 361–428

Weiss R F and Price B A 1980 Nitrous oxide solubility in water and seawater *Mar. Chem.* **8** 347–59

Yang S *et al* 2020 Global reconstruction reduces the uncertainty of oceanic nitrous oxide emissions and reveals a vigorous seasonal cycle *Proc. Natl Acad. Sci.* **117** 201921914

Zamora L M and Oschlies A 2014 Surface nitrification: a major uncertainty in marine N_2O emissions *Geophys. Res. Lett.* **41** 4247–53

Zamora L M, Oschlies A, Bange H, Huebert K, Craig J, Kock A and Löscher C 2012 Nitrous oxide dynamics in low oxygen regions of the Pacific: insights from the MEMENTO database *Biogeosciences* **9** 5007–22

Zickfeld K, Eby M, Matthews H D and Weaver A J 2009 Setting cumulative emissions targets to reduce the risk of dangerous climate change *Proc. Natl Acad. Sci.* **106** 16129–34